

Quasi-Stem Cells Derived from Human Somatic Cells by Chemically Modified Carbon Nanotubes

Jae-Hyeok Lee,*^{†,‡,§,¶} Hyuck-Kwon Kwon,[†] Hyeon-Jun Shin,[†] Gwang-Hyeon Nam,[†] Jae-Ho Kim,[†] and Sangdun Choi^{*,[†]}

[†]Department of Molecular Science and Technology, Ajou University, Suwon 443-749, Republic of Korea

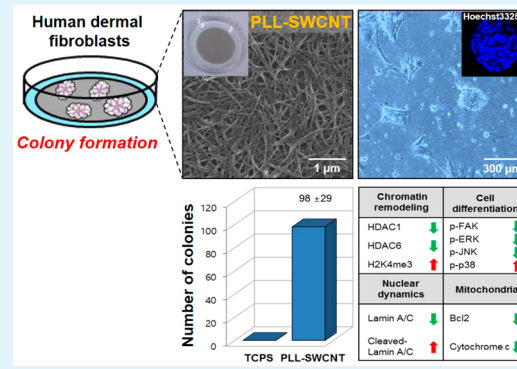
[‡]Department of Materials Science and Engineering, Northwestern University, 2220 Campus Drive, Evanston, Illinois 60208, United States

[§]Predictive Model Research Center, Korea Institute of Toxicology, Daejeon 34114, Republic of Korea

Supporting Information

ABSTRACT: Surface modification of micro- and nanotopography was employed to alter the surface properties of scaffolds for controlling cell attachment, proliferation, and differentiation. This study reports a method for generating multinucleated colonies as evidenced by spherical colony formation through nanotopography-induced expression of reprogramming factors in human dermal fibroblasts. Colony formation was achieved by subjecting the cells to specific environments such as culturing with single-walled carbon nanotubes and poly-L-lysine (PLL-SWCNTs). We obtained encouraging results showing that PLL-SWCNT treatment transformed fibroblast cells, and the transformed cells expressed the pluripotency-associated factors OCT4, NANOG, and SOX2 in addition to TRA-1-60 and SSEA-4, which are characteristic stem cell markers. Downregulation of lamin A/C, HDAC1, HDAC6, Bcl2, cytochrome c, p-FAK, p-ERK, and p-JNK and upregulation of H3K4me3 and p-p38 were confirmed in the generated colonies, indicating reprogramming of cells. This protocol increases the possibility of successfully reprogramming somatic cells into induced pluripotent stem cells (iPSCs), thereby overcoming the difficulties in iPSC generation such as genetic mutations, carcinogenesis, and undetermined risk factors.

KEYWORDS: carbon nanotube, nanotopography, colony formation, quasi-stem cell, stem cell reprogramming factor



1. INTRODUCTION

Embryonic stem cells (ESCs) are pluripotent stem cells derived from blastocysts that have the capacity to differentiate into various cell types or organs of the body.¹ Induced pluripotent stem cells (iPSCs) were developed by Prof. Yamanaka at Kyoto University, Japan in 2006 by overexpressing stem cell specific genes in mouse somatic cells.^{2,3} iPSCs and ESCs share similar morphologies, growth rates, gene expression patterns, and pluripotency potential. The pluripotency of ESC and iPSC, which can differentiate into almost any cell type, is an important factor in stem cell-based therapeutic applications. The use of iPSCs is a way to overcome bioethical concerns and allow the development of stem cells that can be utilized for personalized regenerative cell therapies and various experimental methodologies such as disease modeling, drug screening, and toxicity/efficacy assessment.⁴ However, recent studies on therapeutic development have demonstrated the limitations of iPSCs in clinical applications. For instance, the observed rate of carcinogenesis after iPSCs transplantation in mice was found to be 20%, thereby raising concerns over the use of oncogenes as transcription factors.^{5,6} Critical adverse effects such as carcinogenesis were found to result from

alterations or loss of functions in genes that play important roles in cell processes.^{7,8} Such changes were primarily caused by activation of the Kruppel-like factor 4 (Klf4)⁹ and the cellular myelocytomatosis oncogene (c-Myc),⁵ which are among the Yamanaka factors (Klf4, Oct3/4, c-Myc, and Sox2),² and by random insertion of retroviral gene delivery vectors into host chromosomes.

According to several recent studies, the inherent material properties of the substrate surrounding the cells can determine stem cell fate.^{10,11} For example, the differentiation of human epidermal stem cells can be controlled through nanopatterning by adjusting the stiffness of polyacrylamide.¹² Nanopatterned polydimethylsiloxane (PDMS) was shown to help maintain the self-renewal capacity of mouse ES cells.¹³ Another study reported that expression of OCT4, a pluripotency factor, in human ESC is influenced by the nanotopographical configuration.¹⁴

Received: August 26, 2017

Accepted: December 29, 2017

Published: December 29, 2017



Human ESCs cultured on a plate with hexagonal nanotopography were observed to maintain OCT4 expression without the need for basic fibroblast growth factor (bFGF) supplementation. Moreover, human ESCs cultivated on nanopillars showed higher expression of OCT4, SOX2, and NANOG with decreasing diameter of the nanopillars used for culturing.¹⁵ Mouse embryonic fibroblasts injected with the four reprogramming factors (viz., Oct4, Klf4, Sox2, and c-Myc) and cultured on a microgrooved substrate showed higher levels of histone H3 acetylation and methylation along with a distinct increase in iPSC formation efficiency compared to cells injected only with reprogramming factors.¹⁶ Valproic acid, an inhibitor of Histone deacetylase (HDAC), increased reprogram efficiency and properly induced the properties of pluripotent stem cells without the insertion of c-Myc oncogene.¹⁷ In 2014, human lung fibroblasts treated with carbon nanotubes (CNTs) were demonstrated to undergo colonization and multinucleation and showed increased expression of stem cell surface proteins.^{18,19} Kim et al. demonstrated that mouse iPSC-derived 3D spherical colonies grew well to micro/nanoscale topography of marginally penetrating vertical silicon nanocolumn array substrate and showed enhanced pluripotency activity.²⁰ As a result, new approaches for controlling the epigenetic fate of cells have recently been carefully considered based on the nanotopography of the environment and culture conditions.

As a result of the above-mentioned reports, surface modification of micro- and nanotopography has been used to alter the surface properties of scaffolds to enable the control of cell attachment, proliferation, and differentiation behaviors.

In our previous paper, we studied how changes in the morphological structure of single-walled carbon nanotube (SWCNT) films affect stem cell proliferation and differentiation.²¹ We demonstrated that in contrast to tissue culture polystyrene (TCPS) plates, the prepared SWCNT film-based scaffolds did not exert cytotoxic effects, significantly influenced cell behavior, and promoted differentiation of mesenchymal stem cells (MSCs). Notably, colony formation is one of the distinct features of the produced ESCs or iPSCs.^{22–24} Very recently, we observed that various physiochemical changes in nanotopographical surfaces can influence the cell fate of some stem cells and somatic cells. Surprisingly, our experiments on human MSCs and human dermal fibroblasts (HDFs) showed that these cells could naturally and efficiently undergo spherical colony formation under certain environmental conditions without the introduction of foreign transcription factors or injection of exogenous chemicals. So far, there have been no reports of nanotopography-induced expression of reprogramming factors of stem cells and somatic cells. The use of nanotopography could represent a safer and more efficient means of achieving personalized stem cell therapies because the need for introduction of foreign transcription factors and exogenous chemicals is eliminated.

2. EXPERIMENTAL SECTION

2.1. Chemicals and Materials. For the SWCNTs scaffolds, it is required to prepare a stabilized SWCNT solution. Detailed experimental methods are well-described in our previous paper.²¹ Briefly, 20 mg of arc discharge SWCNTs were dispersed in a strong acid (mixture of HNO_3 and H_2SO_4 , 1:3, v/v, 70 and 98% respectively) using a bath sonicator at 70 °C for 4 h, followed by filtration and neutralization to remove metal catalysts. After acid treatment, the neutralized and chemically carboxylated SWCNTs were dispersed in an aqueous solution containing Triton X-100 surfactant (250 mL, 3 wt %) by ultrasonication for 1 h. Subsequently, a SWCNT suspension was

prepared by centrifugation at 6000 rpm for 1 h and harvesting the supernatant SWCNT suspension. Thiophenyl-modified SWCNTs (SWCNT-SH) were prepared by reacting 4-aminothiophenol with a suspension of carboxy functionalized SWCNTs in 500 mL of *N,N*-dimethylformamide solution.²⁵ Finally, the resulting SWCNT-SH were sonicated in chloroform for 30 min to dissolve, and this solution was used to make the SWCNT scaffold.

2.2. Random Network SWCNT Film on PS Substrate. The SWCNT-SH stock solution (8 mL) was diluted with 50 mL of chloroform and sonicated for 5 min using a bath sonicator. Immediately after sonication, the SWCNT-SH solution was filtered on an alumina oxide (AAO) membrane and then heated in air at 110 °C for 4 h. After annealing, the resulting thin film of SWCNTs on the AAO membrane was carefully placed in an aqueous sodium hydroxide (NaOH) solution (3 M) for 5 h to dissolve the AAO membrane. Upon complete dissolution of AAO membrane, a free-standing random network of SWCNTs remained in the air/water interface. The NaOH solution was then removed using an aspirator, and the SWCNT film was washed with deionized (DI) water to neutral pH (7.0). Finally, the random network SWCNT film was carefully transferred to the PS substrate and heated in air at 93 °C for 10 min.

2.3. PDMS Coating on the Side of the SWCNT Film. To exclude the possibility of cell growth on the PS substrate, PDMS was coated through the edge of the surrounding SWCNT film. The PDMS coating was prepared by mixing a Sylgard 184 Silicon Elastomer (Dow Corning, United States) with a curing agent in a 10:1 ratio. The resulting solution was spread on the area surrounding the SWCNT film using a brush. Finally, the PDMS-coated SWCNT film was heated in air at 93 °C for 10 min.

2.4. Poly-L-lysine (PLL)-Modified SWCNT Film. PLL (M_w : 15 000–30 000, Sigma-Aldrich, United States) was dissolved in phosphate-buffered saline (PBS) solution (0.1 mg/mL). For the preparation of PLL coated SWCNT films, the surface of the nanotube film was immersed in 2 mL of PLL solution at 24 °C for 3 h and then rinsed with DI water. Finally, the PLL-coated SWCNT film was blow-dried with filtered nitrogen.

2.5. Characterization and Instrumentation. The physicochemical characteristics of the prepared SWCNT bundle and network SWCNT films were characterized by scanning electron microscopy (SEM, LEO SUPRA 55, Germany), energy-dispersive X-ray spectroscopy (EDX) analysis of elements (Genesis 2000, EDAX Inc., Mahwah, NJ, United States), and atomic force microscopy (AFM, Park XE-100, South Korea). All AFM images were obtained in noncontact mode using a silicon cantilever (ARROW-NCR probe, NanoWorld Corp., Switzerland) with standard spring constant (42 N/m) and resonance frequency (285–300 kHz) was used in the experiments. The Raman spectrum of the network SWCNT film was measured by confocal Raman system (Acton TriVista CRS, 514.5 nm laser beam). Contact angle measurement was conducted using a Phoenix 150 goniometer (Surface Electro Optics Co. Ltd., Suwon, Korea) following a sessile drop method at room temperature (24 °C).

2.6. Cell Culture. HDFs were obtained from the American Type Culture Collection and cultured in Dulbecco's modified Eagle's medium (DMEM) containing 10% fetal bovine serum (FBS) with 1% antibiotics (penicillin/streptomycin, Thermo Fisher Scientific Inc., Waltham, MA, United States) in humidified atmosphere of 5% CO_2 at 37 °C incubator (Heraeus BB15, United States). Human MSCs derived from bone marrow were purchased from Pharmicell Co. Ltd. (Sungnam, Korea) and grown in StemPro medium (Invitrogen, United States) with 1% penicillin/streptomycin in an incubator. MSCs were purchased from Pharmicell Co. Ltd. (Sungnam, Korea) and grown in StemPro MSC serum-free medium (Invitrogen, Carlsbad, CA, United States) with antibiotics (1% penicillin/streptomycin; Thermo Fisher Scientific Inc., Waltham, MA, United States) in an incubator (humidified atmosphere of 5% CO_2 at 37 °C; Heraeus BB15; Thermo Fisher Scientific Inc.).

2.7. PLL-SWCNT-Induced Colony Formation. HDFs (4×10^5 cells) were seeded on TCPS and/or PLL-SWCNT plates in DMEM without FBS (DMEM), DMEM containing FBS (DMEM + FBS), and mTeSR1 (STEMCELL Technology, Vancouver, BC, Canada)

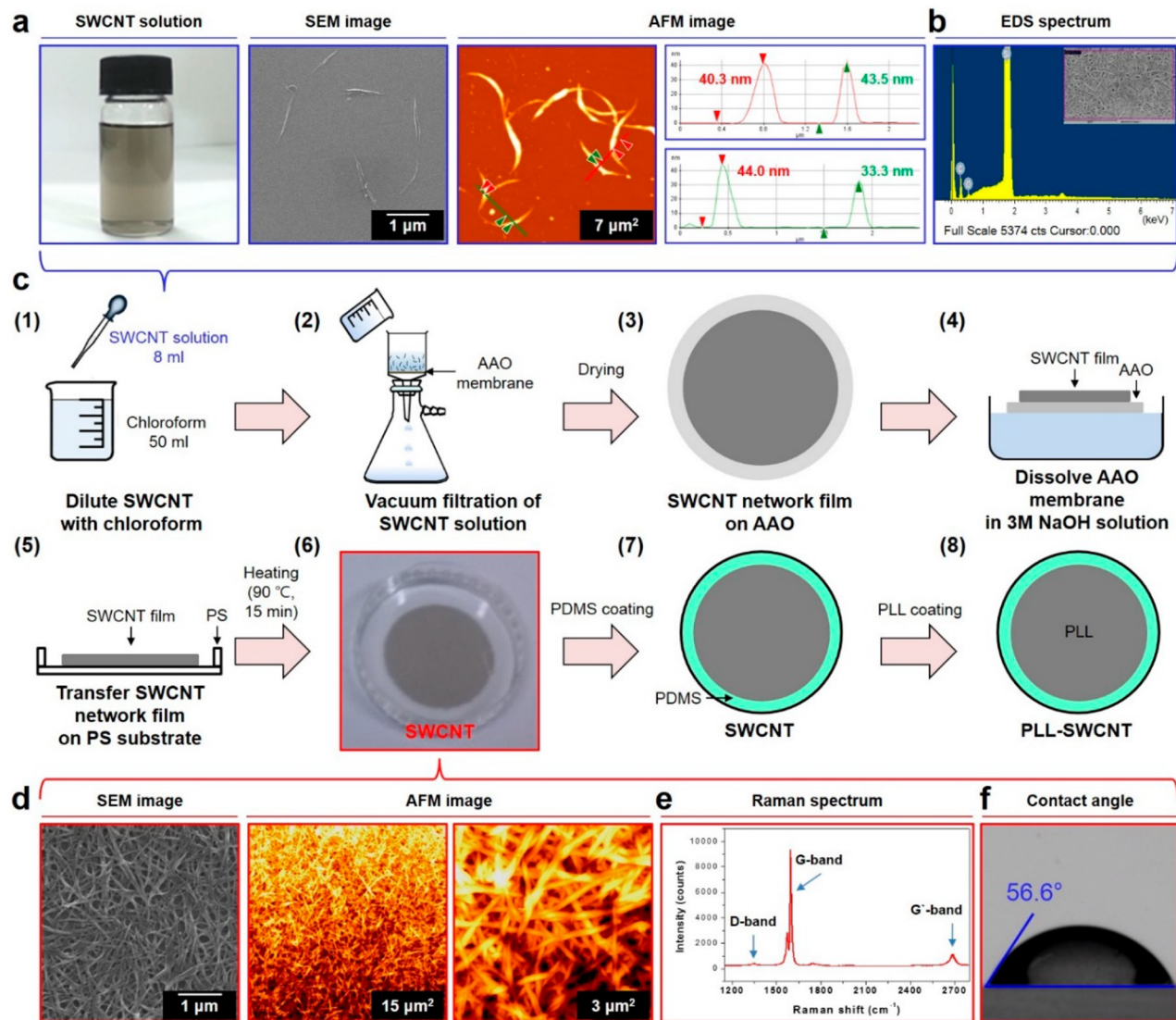


Figure 1. Schematic illustration of fabrication procedure of poly-L-lysine coated random network SWCNT films. (A) The geometrical structure of the SWCNT bundle was evaluated by SEM and AFM measurements. Images show a homogeneous solution of thiophenyl-modified SWCNTs in CHCl₃, and SEM and AFM images of uniform fibrous SWCNT bundles. The bundle diameters of SWCNTs were measured based on the height profile of the AFM images. (B) EDX spectrum of the purified SWCNT films on silicon substrate, showing that SWCNTs contain carbon, oxygen, and silicon, as expected. (C) Schematic diagram of sequential fabrication procedure of random network SWCNT films. SWCNT films were manufactured by vacuum filtration and transferred onto the PS region, and PLL was subsequently coated on the SWCNT region. (D) Well-constructed random network SWCNT films were evaluated using SEM and AFM. Bars denote the image resolution. (E) Typical Raman peaks of purified SWCNTs were detected using the disorder induced D-band (1350 cm⁻¹), tangential G-band (1573 cm⁻¹), and second-order G'-band (2687 cm⁻¹) on a Raman measurement system (514.5 nm excitation line). (F) Surface wettability of the PLL-coated SWCNT film was measured using a water contact angle measurement system.

medium for 5 days added with an 1% antibiotic cocktail (penicillin/streptomycin) in humidified atmosphere of 5% CO₂ at 37 °C incubator. MSCs (4 × 10⁵ cells) were plated on tissue culture TCPS and/or PLL-SWCNT plates in StemPro MSC serum-free medium (Invitrogen) added with antibiotic cocktail (1% penicillin/streptomycin) for 3 days in an incubator (5% CO₂ at 37 °C). Morphological changes were evaluated by phase-contrast microscopy and analyzed using ScopePhoto software (DCM130; Hangzhou Scopetek Opto-Electric Co. Ltd. Zhejiang, China).

2.8. Real-Time PCR of Genes Influencing Stem Cell Characteristic Physiology. Total RNA was obtained using the QuickGene SP kit (Fujifilm, Tokyo, Japan), and the extracts were quantified in a micro UV-vis fluorescence spectrophotometer. The extracted total RNA was converted into cDNA using commercially available QuantiTect Reverse Transcription Kit. Real-time PCR was carried out using Maxima SYBR Green/ROX qPCR Master Mix on a

real-time ERK cycler (Bio-Rad Laboratories, United States) with primers for OCT4, NANOG, c-MYC, SOX2, KLF4, and glyceraldehyde 3-phosphate dehydrogenase (GAPDH) following a previously described protocol.^{26,27} Relative mRNA expression levels were calculated using the $\Delta\Delta^{CT}$ method. mRNA levels of the target genes were normalized against GAPDH.

2.9. Confocal Microscopy Analysis of Molecules Associated with Stem Cell Biology. HDFs (4 × 10⁵ cells) on PLL-SWCNT were fixed with formaldehyde (3.7%, for 15 min), and permeability was maintained for 15 min with 0.2% Triton X-100 in PBS. Cells were blocked for 1 h in 5% FBS in PBS and then incubated overnight at 4 °C with specific primary antibodies (1:1000) against NANOG, SOX2, SSEA-4, and TRA-1-60 (Abcam, Cambridge, MA, United States). After incubation, the cells were washed at least three times in PBST (0.05% Tween-20 in PBS) and incubated with Alexa Fluor 488 or 546 labeled secondary antibodies (1:1000) for 1 h. Nuclei were stained with

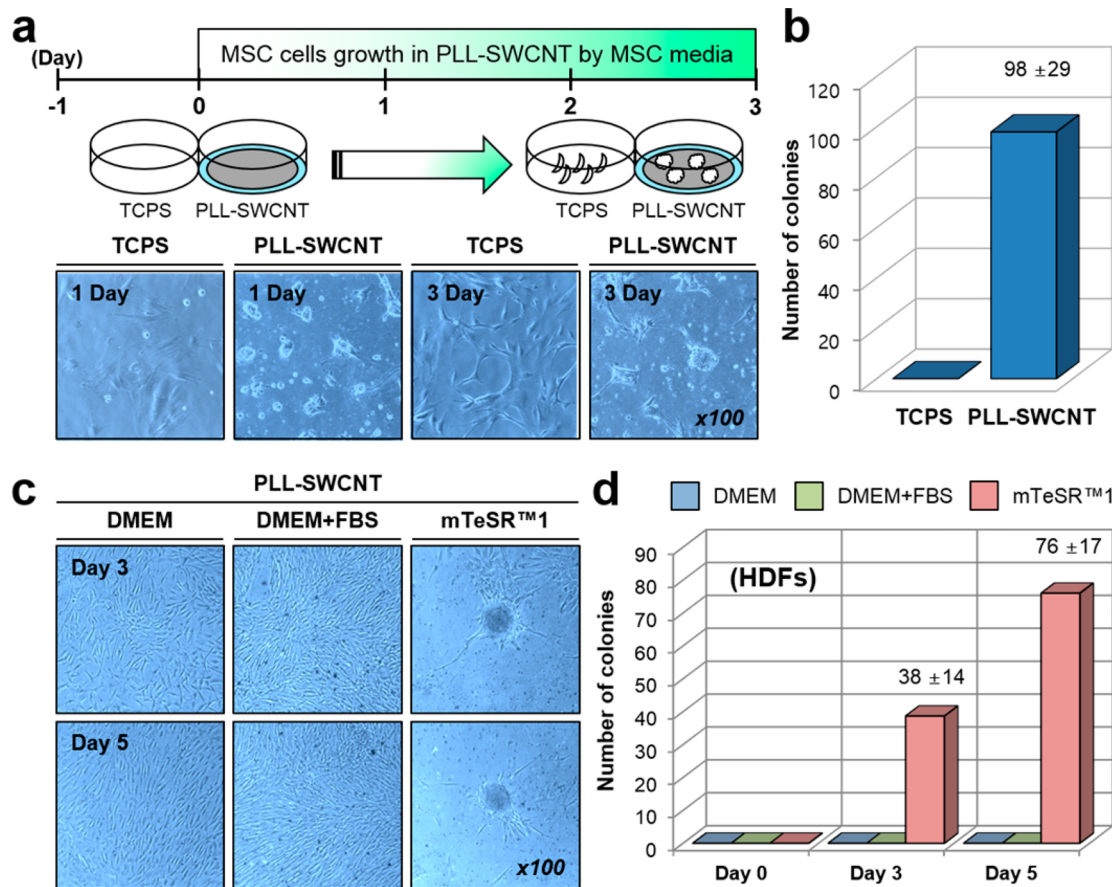


Figure 2. Colony formation in cells cultured in PLL-SWCNTs. (A and B) Human MSCs were seeded on plates of PLL-SWCNT. (A) Morphological changes in human MSCs were investigated in multiple cases using phase contrast microscopy on days 1 and 3. (B) The number of colonies that formed were counted on days 3 and 5. (C and D) HDFs were seeded on PLL-SWCNT plates and cultured with various media, including DMEM without FBS, DMEM containing FBS (DMEM + FBS), or mTeSR1 medium. (C) Morphological changes were investigated using phase contrast microscopy on days 3 and 5. (D) Colonies were counted in PLL-SWCNT plates with the various culture media. All data were obtained from results of at least three individual experiments.

Hoechst33258 reagent ($5 \mu\text{M}$; Sigma-Aldrich) for 15 min. Stained cells were imaged using confocal microscopy.

2.10. Western Blotting Analysis. HDFs (4×10^5 cells) were grown on TCPS and PLL-coated on PS, SWCNT, and PLL-SWCNT for 5 days. Cells were then collected by trypsinization for 5 min and collected via centrifugation at 200g for 5 min. Whole proteins were extracted using M-PER solution following the manufacturer's guidelines (Thermo Fisher Scientific Inc.). Protein concentrations were calculated using the bicinchoninic acid assay (Sigma-Aldrich) following to manufacturer's guidelines. Equal amounts of proteins were separated using a gel electrophoresis system. Subsequently, proteins were transferred to nitrocellulose membranes in transfer buffer using a Mini Trans-Blot (condition; at 70 V for 4 h at 4 °C, Bio-Rad Laboratories). Nitrocellulose membranes were blocked with 0.05% nonfat dried milk solution in DI water for 1 h on a shaker (SH30; Fine PCR, Korea). Immunoblotting was performed using specific primary antibodies (1:1000) against cleaved caspase 3, lamin A/C, Bcl2, cytochrome C, β-actin, p-ERK, p-P38 (Santa Cruz Biotechnology, United States), HDAC1, HDAC6, p-JNK (EMD Millipore Corporation, Temecula, CA, United States), H3K4me3, H3, p-FAK, and GAPDH overnight at 4 °C. The next day, nitrocellulose membranes were washed at least thrice with PBST and incubated with peroxidase-conjugated antirabbit or antimouse antibodies for 2 h. Protein levels were measured using SuperSignal West Pico ECL.

2.11. Statistical Analysis. For reproducibility of the experiments, statistical analyses were performed on three or more identical experimental data. Results were considered statistically significant at $*P < 0.05$ or $**P < 0.01$ based on ANOVA (one-way analysis of

variance) using SigmaPlot software (Version 12.0, Systat Software Inc., United States).

3. RESULTS AND DISCUSSION

First, we fabricated tissue culture plates containing random network SWCNT films coated with PLL. Commercially available carbon nanotubes generally contain high levels of carbonaceous impurities and metal catalysts such as amorphous carbon, Fe, Ni, and Co.²⁸ The presence of these impurities in the CNTs leads to toxicity in nanobio applications.²⁹ Consequently, acid purification of CNTs followed by appropriate surface modifications for stabilization is critical for CNT-based biological applications. In this study, SWCNTs-based tissue culture plates were prepared using a dispersion of chemically well-dispersed SWCNTs (thiophenyl-modified SWCNTs) in chloroform (0.2 mg/L). SWCNTs have rigid rod-like structures with an average diameter of 40.0 ± 5.0 nm and length of $1.5 \pm 0.2 \mu\text{m}$ and lack impurities and metal catalysts (Figure 1A). The EDX data of SWCNT networks mainly showed carbon and oxygen peaks from SWCNTs, indicating that most of the metals were removed by the purification process (Figure 1B). Figure 1C summarizes the procedure for preparing PLL-SWCNTs on a PS substrate, which employs vacuum filtration and transfer methods. The random network SWCNT film was then transferred and

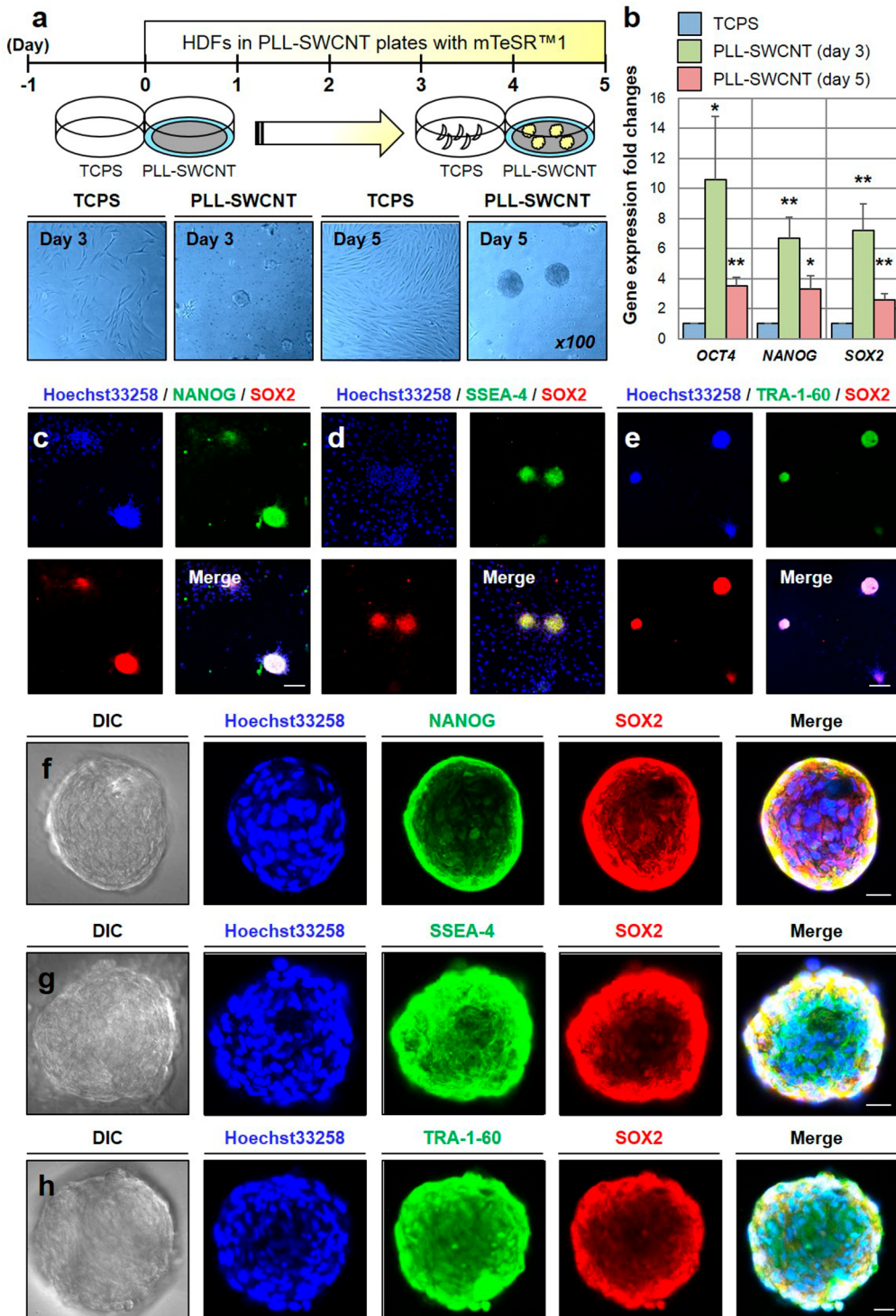


Figure 3. PLL-SWCNTs induced the expression of pluripotency factors and stem cell surface markers. HDFs were seeded on PLL-SWCNT plates and cultured in mTeSR1 medium. (A) Colony formation was detected in cells cultured in PLL-SWCNT plates but not in cells cultured in TCPS plates with mTeSR1 medium. (B) Expression levels of genes encoding pluripotency factors such as OCT4, NANOG, and SOX2 were measured via RT-PCR system. (C–H) The formation of multinuclei was observed using Hoechst33258 staining (blue); significant upregulation of NANOG (green; C and F), SOX2 (red; C–H), SSEA-4 (green; D and G), and TRA-1-60 (green; E and H) was observed with confocal microscopy. Differential interference contrast microscopy showed the formation of colonies. Scale bars indicate 100 μ m (C–E) and 20 μ m (F–H). All data were obtained from the results of at least three individual experiments.

attached to the PS surface by heat treatment at 93 °C for 10 min.³⁰ Without heating, the network detaches from the substrate over time during cell growth. SEM and AFM analyses of the resulting SWCNT films showed that the CNTs were

uniformly distributed, as shown in Figure 1C. The surrounding edges of the SWCNT films were coated with PDMS to produce a PS region without SWCNTs unavailable for cell growth. SWCNT network film was coated with PLL to facilitate cell

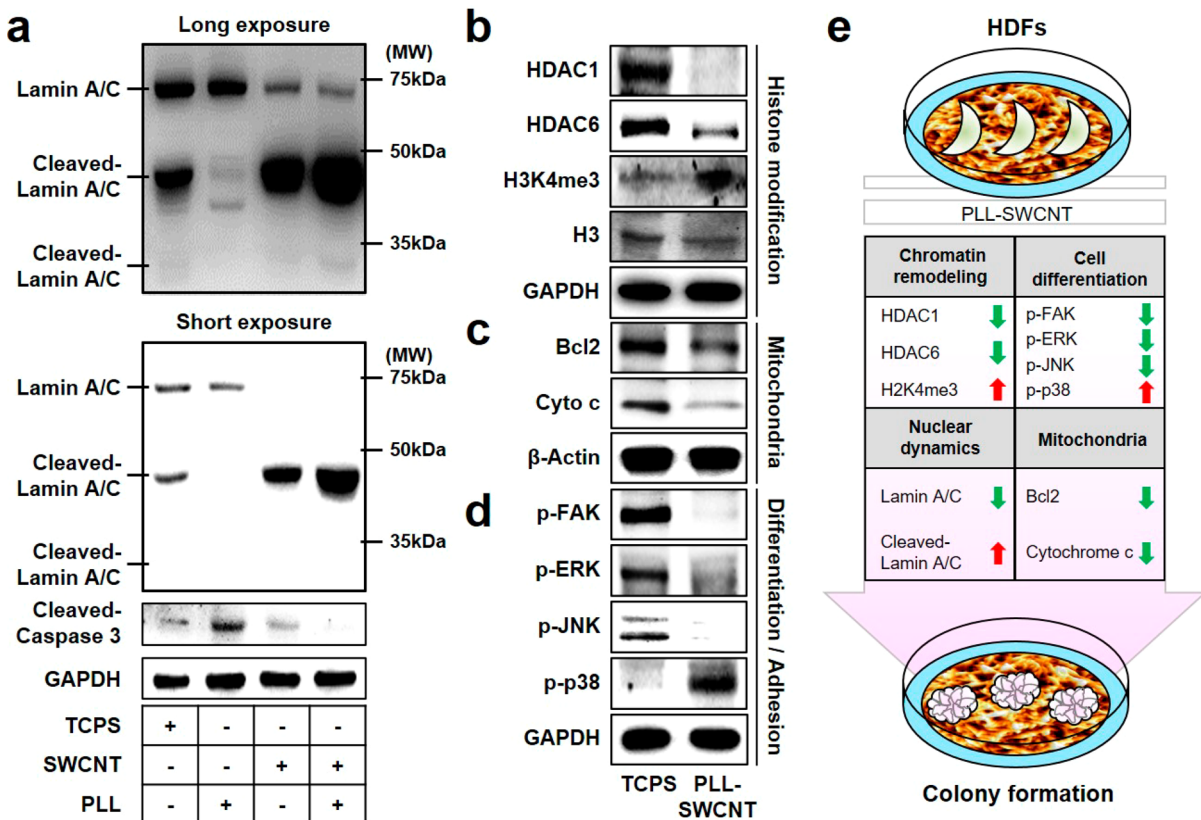


Figure 4. PLL-SWCNTs strongly induced the expression of reprogramming factors. (A) Protein expression levels of lamin A/C, cleaved lamin A/C, and cleaved caspase 3 were measured by Western blotting of whole extracts from HDF cultured in various conditions (TCPS; tissue culture polystyrene, SWCNT; single-walled carbon nanotube, PLL; poly-L-lysine) with mTeSR1 medium for 5 days. GAPDH was used as a loading control. (B) Expression levels of histone modification proteins, histone deacetylase 1 (HDAC1) and HDAC6, and trimethylation of histone H3 Lys 4 (H3K4me3) were measured by Western blotting in the whole extracts from HDF cultured in mTeSR1 medium for 5 days. Histone H3 and GAPDH were used as loading controls. (C) Expression of mitochondrial proteins, including Bcl2 and cyto c, were measured by Western blotting analysis (β -actin was a loading control). (D) Differentiation- and adhesion-related proteins, including p-FAK, p-JNK, p-ERK, and p-p38 measured by Western blotting analysis (GAPDH was a loading control). (A–D) Full-length gels and blots are included in Figure S4. (E) Influence of PLL-SWCNTs on the expression of reprogramming factors and colony formation. All data were obtained from the results of at least three individual experiments.

attachment (Figure 1D). For qualitative characterization and to confirm the wetting property of SWCNTs, Raman spectroscopy and contact angle measurements were performed. The typical Raman peaks of SWCNT were detected with D, G, and G' bands at 1350, 1573, and 2687 cm^{-1} , respectively (Figure 1E). For wettability, the average water contact angle of the network SWCNT film was 56.6° and about 55.7° for the PLL coated SWCNT film (PLL-SWCNT) (Figure 1F and Figure S1a inset, Supporting Information). These results indicate that surface modification of SWCNTs can provide hydrophilic properties suitable for cell culture. The stiffness of the PLL-SWCNT film was measured using a force and distance (F/D) curve-mode of AFM.³¹ The F/D curve-mode of AFM is used to measure the mechanical properties (adhesion, Young's modulus, etc.) of the sample. Especially, estimation of Young's modulus from the F/D curve provides the stiffness information for the sample. In the present study, we also measured the stiffness of PLL-SWCNT film using the F/D curve-mode of AFM. As a result, we demonstrated that the average ($n = 3$) PLL-SWCNT film stiffness was about 14.87 MPa (Figure S1b).

Differentiation patterns of human MSCs cultured in PLL-SWCNT plates include morphological changes in some of the cells and eventual colony formation under specific conditions (Figure 2A). Colony formation is one of the initial characteristics of iPSCs. As shown in Figure 2B, the use of PLL-

SWCNTs resulted in a significantly higher number of colonies formed than tissue culture polystyrene (TCPS) after three days of culture. Thus, HDFs were seeded in PLL-SWCNT plates in further experiments. Cells were cultured using DMEM without FBS, DMEM containing FBS, and mTeSR1. No morphological changes were observed in HDFs grown in PLL-SWCNT plates with DMEM or DMEM + FBS after three or five days (Figure 2C). By contrast, HDFs cultured in PLL-SWCNT plates with mTeSR1 medium showed colony formation and morphological changes that are characteristic of iPSCs. Colony formation in cells cultured in PLL-SWCNT plates with mTeSR1 medium significantly increased over time, whereas cells grown in the two other media did not exhibit colony formation (Figure 2D). mTeSR1, a serum-free medium objected for the feeder-free culture of human ESCs, contains five factors [bFGF, transforming growth factor beta (TGF- β), gamma-aminobutyric acid (GABA), lithium chloride, and pipecolic acid] that promote and maintain the proliferation of undifferentiated human stem cells.³²

Colonization of HDF cells was investigated on various types of plates (TCPS, SWCNT, PLL coated TCPS, and PLL-SWCNT) (Figure S2). mTeSR1 medium was used for HDF cell culture. Cells on TCPS and SWCNT (without PLL) presented normal cell proliferation. PLL coated TCPS triggered cell aggregation but not formed colonies. As a result, these data

showed TCPS, PLL coated TCPS, and SWCNT (without PLL) substrates did not induce colony formation except for the PLL-SWCNT substrate in same media (mTeSR1). This means that the role of PLL and specific cell culture conditions (PLL-SWCNT + mTeSR1) play a crucial role in the formation of colonies rather than the effect of SWCNT itself.

ESC and iPSC are uniquely characterized by cell colony formation with multiple nuclei and exhibit high expression of pluripotency-related molecules (OCT4, SOX2, NANOG, KLF4, and c-MYC) and stem cell surface markers such as SSEA-4 and TRA-1-60.³³ As shown in Figure 3A, culturing HDFs in PLL-SWCNT plates with mTeSR1 medium induced colony formation at around day 3. However, HDFs cultured in TCPS plates with mTeSR1 medium did not produce colonies until day 5 (Figure 3A). RT-PCR analyses showed significant upregulation of OCT4, NANOG, and SOX2 in cells cultured in PLL-SWCNT plates compared to cells cultured in TCPS (Figure 3B). Expression of c-MYC and KLF4, which are known oncogenes, was not detected (for c-MYC) or was barely detected (for KLF4; detection only occurred after 35 or 36 amplification cycles under RT-PCR conditions described in the Experimental Section) in all samples tested. Confocal immunofluorescence microscopy analyses showed morphological changes over time, as indicated by colonization and multinucleation, upregulation of pluripotency factors such as NANOG and SOX2 (Figures 3C and F), and expression of the stem cell surface markers SSEA-4 (Figures 3D and G) and TRA-1-60 (Figures 3E and H). However, pluripotency factors and stem cell surface markers were weakly expressed in the progressing colony-forming cells and absent in noncolony-forming cells (Figures 3C–E). Furthermore, OCT4 and NANOG expression levels were measured by immunofluorescence staining and detected using confocal microscopy analysis (Figure S3). Interestingly, this result showed that NANOG was strongly stained in the nucleus which colocalized with nucleus dye. In the case of OCT4, the level of expression was definitely increased in cytosol, but it was weakly expressed in nucleus as a result of 3D image and line profile analysis. These results suggest that HDF can be reprogrammed into pluripotent stem cells under the well-designed environmental conditions described here.

Lamin A/C, which has almost the same amino acid sequence, is a scaffolding component of mammal nuclei, mainly expressed in differentiated cells and functions in cell maintenance, not ESC or iPSC.^{34–36} However, a previous report showed that mouse ESCs express low levels of the transcripts of both isoforms.³⁷ In our study, reduced expression of lamin A/C was observed in cells cultured in SWCNTs or PLL-SWCNT plates, indicating a transition from a differentiated state into iPSCs (Figure 4A). Intriguingly, the expression of cleaved lamin A/C (45 kDa; large subunit) was significantly increased in cells grown in SWCNT and PLLSWCNT plates. This pattern may reflect extensive architectural changes in the nuclear envelope in stem cells undergoing rapid self-renewal through mitosis. Western blotting results showed no activation of caspase 3 in cells grown in SWCNT or PLL-SWCNT plates (Figure 4A). As an important example, research has recently been reported to increase the efficiency of iPSC production when injected with a broad class I and II histone deacetylase (HDAC) inhibitor, valproic acid, and transcription factors (Oct4, Klf4, Sox2, and c-Myc).^{17,38} Decreased HDAC activity leads to increased histone H3 acetylation, which increases the expression of a new set of genes. The pluripotent states of both ESCs and iPSCs are

characterized by trimethylation of histone H3 Lys 4 (H3K4me3).³⁹ In our study, downregulation of HDAC1 and upregulation of H3K4me3 were confirmed through Western blot analysis (Figure 4B), suggesting that modulation of the epigenetic state may be responsible for the transition of HDFs into a pluripotent state. B-cell lymphoma 2 (Bcl2) is localized to the outer membrane of mitochondria and plays a crucial role in the antiapoptotic process.^{40,41} Under apoptotic stimulation, permeabilization of mitochondrial membrane induces cytochrome c (cyt c) from the inner membrane of mitochondria, but does not change overall expression levels.⁴¹ Compared to differentiated cells, pluripotent stem cells contain a smaller number of mitochondria and fewer copies of mitochondrial DNA as well as reduced ATP production and oxidative phosphorylation.⁴² Our results clearly showed that cells grown in PLL-SWCNT plates exhibit lower expression of Bcl2 and cyt c compared with those cultured in TCPS (Figure 4C).

Most cells in the human body, except for blood cells, are attached to the extracellular matrix (ECM), which is composed of proteins and polysaccharides in vivo. The ECM appropriately supplies the biochemical factors necessary for cell growth and differentiation while providing appropriate physiological conditions for the cells. In addition, ECM plays a very important role as a cell-mediated ligand and physiological regulator of processes such as cell division, differentiation, and death. Notably, cell adhesion to the ECM can be indicated by focal adhesions (FAs) assembly that fixes the actin cytoskeleton to the ECM and induces signaling for cell growth and migration.⁴³ Especially, the SWCNTs produced in this study form rigid rod-like structures (diameter: 40.0 ± 5.0 nm; length: $1.5 \pm 0.2 \mu\text{m}$) and are able to form nanofibrous networks with surface roughness of ~ 10 nm, which is similar to that of the ECM structure. In our previous study, we demonstrated that morphological changes and hydrophilic surface properties of network SWCNT films (similar to ECM network structure) have a positive impact on MSC growth and differentiation.²¹ Recently, Jaggy et al. reported long-term self-renewal characteristics of mESC over three weeks using hierarchical micro/nano surface roughness (MN surface) and showed that only MN surface induces actin-positive cell protrusion. These results indicate that the substrate structures are related to the mechanism by which the characteristics of the mESC stemness are maintained.⁴⁴ Here, we showed for the first time a novel cell culture substrate that can induce and maintain colony formation of human dermal fibroblast cells based on the physicochemical properties (nanoscale surface roughness) of the PLL-SWCNT. To study the relationship between the substrate and the cell, we investigated and analyzed the gene closely related to the FAs. Interaction of nanotopographical shapes with integrin receptors in FAs of cells determines cell fate.⁴⁵ Absence of the phosphorylated form of focal adhesion kinase (FAK), which is important for cell differentiation and adhesion, along with downregulation of the phosphorylated forms of downstream signaling proteins such as c-Jun N-terminal kinase (JNK) and extracellular signal regulated kinase (ERK),⁴⁶ was observed (Figure 4D). Activation of the ERK and JNK pathways blocks the induction of dedifferentiation into iPSCs.^{47,48} Phosphorylated p38 levels were found to be upregulated (Figure 4D). p38 activation mediated by environmental stress can promote reprogramming by reducing the degree of DNA methylation levels and increasing the expression of pluripotency.⁴⁸ All the results are consistent with the previously reported characteristic outcomes for iPSCs.

4. CONCLUSIONS

In the present study, we introduced the concept of cell reprogramming induced by the cell culture conditions (Figure 4E). Culturing human dermal fibroblast cells in a specific environment containing SWCNTs and PLLs produced cells with morphological and molecular properties identical to those of currently used pluripotent stem cell types without the need for introducing foreign transcription factors. Compared to general methods that utilize foreign transcription factors such as OCT4, NANOG, and SOX2, the expression level of pluripotency factors by nanotopography was relatively low. However, nanotopography showed effects similar to those of chemicals that modulate numerous important reprogramming factors for iPSC generation. Taken together, this method can generate iPSCs by altering the nanotopography of the culture environment. Therefore, this method represents a safe and effective method to produce stem cells that can be applied in human clinical therapy.

■ ASSOCIATED CONTENT

Supporting Information

The Supporting Information is available free of charge on the ACS Publications website at DOI: [10.1021/acsami.7b12914](https://doi.org/10.1021/acsami.7b12914).

(SI-1) AFM image and F/D curve of PLL-SWCNT film measured by AFM (a and b); wettability of PLL-SWCNT film; (SI-2) optical images of HDFs cultured on various types of plates; (SI-3) Oct4 and NANOG expression patterns in HDF colonies; and (SI-4) PLL-SWCNT coated plate which altered the various signaling proteins ([PDF](#))

■ AUTHOR INFORMATION

Corresponding Authors

*E-mail: jaehyeok.lee@kitox.re.kr.

*E-mail: sangdunchoi@ajou.ac.kr.

ORCID

Jae-Hyeok Lee: [0000-0003-0559-6256](https://orcid.org/0000-0003-0559-6256)

Author Contributions

J.-H.L., H.-K.K., H.-J.S., and S.C. conceived the study and designed the experiments. J.-H.L., H.-K.K., H.-J.S., and G.-H.N. performed the experiments. J.-H.L., H.-K.K., H.-J.S., and S.C. analyzed the data. J.-H.K. and S.C. contributed material. J.-H.L., H.-K.K., H.-J.S., and S.C. wrote the manuscript. J.-H.L., H.-K.K., and H.-J.S. contributed equally to this work.

Notes

The authors declare no competing financial interest.

■ ACKNOWLEDGMENTS

This research was supported by a grant from the Korea Health Technology R&D Project through the Korea Health Industry Development Institute (Grant HI14C1992) and the National Research Foundation of Korea (Grant NRF-2015R1A2A2A09001059). In addition, this study was partially supported by a grant from the Priority Research Centers Program (Grant NRF 2012-0006687).

■ REFERENCES

- (1) Martin, G. R. Isolation of a Pluripotent Cell Line from Early Mouse Embryos Cultured in Medium Conditioned by Teratocarcinoma Stem Cells. *Proc. Natl. Acad. Sci. U. S. A.* **1981**, *78*, 7634–7638.

- (2) Takahashi, K.; Yamanaka, S. Induction of Pluripotent Stem Cells from Mouse Embryonic and Adult Fibroblast Cultures by Defined Factors. *Cell* **2006**, *126*, 663–676.
- (3) Takahashi, K.; Yamanaka, S. A Decade of Transcription Factor-Mediated Reprogramming to Pluripotency. *Nat. Rev. Mol. Cell Biol.* **2016**, *17*, 183–193.
- (4) Robinton, D. A.; Daley, G. Q. The Promise of Induced Pluripotent Stem Cells in Research and Therapy. *Nature* **2012**, *481*, 295–305.
- (5) Okita, K.; Ichisaka, T.; Yamanaka, S. Generation of Germline-Competent Induced Pluripotent Stem Cells. *Nature* **2007**, *448*, 313–317.
- (6) Ben-David, U.; Benvenisty, N. The Tumorigenicity of Human Embryonic and Induced Pluripotent Stem Cells. *Nat. Rev. Cancer* **2011**, *11*, 268–277.
- (7) Wasik, A. M.; Grabarek, J.; Pantovic, A.; Cieslar-Pobuda, A.; Asgari, H. R.; Bundgaard-Nielsen, C.; Rafat, M.; Dixon, I. M.; Ghavami, S.; Los, M. J. Reprogramming and Carcinogenesis-Parallels and Distinctions. *Int. Rev. Cell Mol. Biol.* **2014**, *308*, 167–203.
- (8) Nishimori, M.; Yakushiji, H.; Mori, M.; Miyamoto, T.; Yaguchi, T.; Ohno, S.; Miyake, Y.; Sakaguchi, T.; Ueda, M.; Ohno, E. Tumorigenesis in Cells Derived from Induced Pluripotent Stem Cells. *Hum. Cell* **2014**, *27*, 29–35.
- (9) Leng, Z.; Tao, K.; Xia, Q.; Tan, J.; Yue, Z.; Chen, J.; Xi, H.; Li, J.; Zheng, H. Kruppel-Like Factor 4 Acts as an Oncogene in Colon Cancer Stem Cell-Enriched Spheroid Cells. *PLoS One* **2013**, *8*, e56082.
- (10) Murphy, W. L.; McDevitt, T. C.; Engler, A. J. Materials as Stem Cell Regulators. *Nat. Mater.* **2014**, *13*, 547–557.
- (11) Higuchi, A.; Ling, Q. D.; Suresh Kumar, S.; Chang, Y.; Alarfaj, A. A.; Munusamy, M. A.; Murugan, K.; Hsu, S.-T.; Umezawa, A. Physical Cues of Cell Culture Materials Lead the Direction of Differentiation Lineages of Pluripotent Stem Cells. *J. Mater. Chem. B* **2015**, *3*, 8032–8058.
- (12) Trappmann, B.; Gautrot, J. E.; Connelly, J. T.; Strange, D. G.; Li, Y.; Oyen, M. L.; Cohen Stuart, M. A.; Boehm, H.; Li, B.; Vogel, V.; Spatz, J. P.; Watt, F. M.; Huck, W. T. Extracellular-Matrix Tethering Regulates Stem-Cell Fate. *Nat. Mater.* **2012**, *11*, 642–649.
- (13) Jeon, K.; Oh, H. J.; Lim, H.; Kim, J. H.; Lee, D. H.; Lee, E. R.; Park, B. H.; Cho, S. G. Self-Renewal of Embryonic Stem Cells through Culture on Nanopattern Polydimethylsiloxane Substrate. *Biomaterials* **2012**, *33*, 5206–5220.
- (14) Kong, Y. P.; Tu, C. H.; Donovan, P. J.; Yee, A. F. Expression of Oct4 in Human Embryonic Stem Cells is Dependent on Nanotopographical Configuration. *Acta Biomater.* **2013**, *9*, 6369–6380.
- (15) Bae, D.; Moon, S. H.; Park, B. G.; Park, S. J.; Jung, T.; Kim, J. S.; Lee, K. B.; Chung, H. M. Nanotopographical Control for Maintaining Undifferentiated Human Embryonic Stem Cell Colonies in Feeder Free Conditions. *Biomaterials* **2014**, *35*, 916–928.
- (16) Downing, T. L.; Soto, J.; Morez, C.; Houssin, T.; Fritz, A.; Yuan, F.; Chu, J.; Patel, S.; Schaffer, D. V.; Li, S. Biophysical Regulation of Epigenetic State and Cell Reprogramming. *Nat. Mater.* **2013**, *12*, 1154–1162.
- (17) Huangfu, D.; Maehr, R.; Guo, W.; Eijkelenboom, A.; Snitow, M.; Chen, A. E.; Melton, D. A. Induction of Pluripotent Stem Cells by Defined Factors is Greatly Improved by Small-Molecule Compounds. *Nat. Biotechnol.* **2008**, *26*, 795–797.
- (18) Luanpitpong, S.; Wang, L.; Manke, A.; Martin, K. H.; Ammer, A. G.; Castranova, V.; Yang, Y.; Rojansakul, Y. Induction of stemlike cells with fibrogenic properties by carbon nanotubes and its role in fibrogenesis. *Nano Lett.* **2014**, *14*, 3110–3116.
- (19) Luanpitpong, S.; Wang, L.; Castranova, V.; Rojansakul, Y. Induction of Stem-Like Cells with Malignant Properties by Chronic Exposure of Human Lung Epithelial Cells to Single-Walled Carbon Nanotubes. *Part. Fibre Toxicol.* **2014**, *11*, 22.
- (20) Kim, H.; Kang, D. H.; Koo, K. H.; Lee, S.; Kim, S. M.; Kim, J.; Yoon, M. H.; Kim, S. Y.; Yang, E. G. Vertical Nanocolumn-Assisted Pluripotent Stem Cell Colony Formation with Minimal Cell-Penetration. *Nanoscale* **2016**, *8*, 18087–18097.

- (21) Lee, J. H.; Shim, W.; Choolakadavil Khalid, N.; Kang, W. S.; Lee, M.; Kim, H. S.; Choi, J.; Lee, G.; Kim, J. H. Random Networks of Single-Walled Carbon Nanotubes Promote Mesenchymal Stem Cell's Proliferation and Differentiation. *ACS Appl. Mater. Interfaces* **2015**, *7*, 1560–1567.
- (22) Lee, G.; Papapetrou, E.; Kim, H.; Chambers, S.; Tomishima, M.; Fasano, C.; Ganat, Y.; Menon, J.; Shimizu, F.; Viale, A.; Tabar, V.; Sadelain, M.; Studer, L. Modeling Pathogenesis and Treatment of Familial Dysautonomia using Patient Specific iPSCs. *Nature* **2009**, *461*, 402–406.
- (23) Chen, G.; Gulbranson, D.; Hou, Z.; Bolin, J.; Ruotti, V.; Probasco, M.; Smuga-Otto, K.; Howden, S.; Diol, N.; Propson, N.; Wagner, R.; Lee, G.; Antosiewicz-Bourget, J.; Teng, J.; Thomson, J. Chemically Defined Conditions for Human iPS Cell Derivation and Culture. *Nat. Methods* **2011**, *8*, 424–429.
- (24) Warren, L.; Manos, P.; Ahfeldt, T.; Loh, Y. H.; Li, H.; Lau, F.; Ebina, W.; Mandal, P.; Smith, Z.; Meissner, A.; Daley, G.; Brack, A.; Collins, J.; Cowan, C.; Schlaeger, T.; Rossi, D. Highly Efficient Reprogramming to Pluripotency and Directed Differentiation of Human Cells with Synthetic Modified mRNA. *Cell Stem Cell* **2010**, *7*, 618–630.
- (25) Lee, J. H.; Kang, W. S.; Nam, G. H.; Choi, S. W.; Kim, J. H. Preparation of Hierarchically Aligned Carbon Nanotube Films Using the Langmuir-Blodgett Technique. *J. Nanosci. Nanotechnol.* **2009**, *9*, 7080–7084.
- (26) Yu, J.; Vodyanik, M. A.; Antosiewicz-Bourget, J.; Frane, J. L.; Tian, S.; Nie, J.; Jonsdottir, G. A.; Ruotti, V.; Stewart, R.; Slukvin, I. I.; Thomson, J. A. Induced Pluripotent Stem Cell Lines Derived from Human Somatic Cells. *Science* **2007**, *318*, 1917–1920.
- (27) Deb-Rinker, P.; Ly, D.; Jezierski, A.; Sikorska, M.; Walker, P. R. Sequential DNA Methylation of the Nanog and Oct-4 Upstream Regions in Human NT2 Cells during Neuronal Differentiation. *J. Biol. Chem.* **2005**, *280*, 6257–6260.
- (28) Journet, C.; Maser, W. K.; Bernier, P.; Loiseau, A.; Lamy de la Chapelle, M.; Lefrant, S.; Deniard, P.; Lee, R.; Fischer, J. E. Large-scale production of single-walled carbon nanotubes by the electric-arc technique. *Nature* **1997**, *388*, 756–758.
- (29) Lam, C. W.; James, J. T.; McCluskey, R.; Arepalli, S.; Hunter, R. L. A Review of Carbon Nanotube Toxicity and Assessment of Potential Occupational and Environmental Health Risks. *Crit. Rev. Toxicol.* **2006**, *36*, 189–217.
- (30) Qu, L.; Dai, L.; Stone, M.; Xia, Z.; Wang, Z. L. Carbon Nanotube Arrays with Strong Shear Binding-On and Easy Normal Lifting-Off. *Science* **2008**, *322*, 238–242.
- (31) Kwon, C.; Chun, K. Y.; Kim, S.; Lee, J. H.; Kim, J. H.; Lima, M.; Baughman, R.; Kim, S. Torsional Behaviors of Polymer-infiltrated Carbon Nanotube Yarn Muscles Studied with Atomic Force Microscopy. *Nanoscale* **2015**, *7*, 2489–2496.
- (32) Ludwig, T. E.; Levenstein, M. E.; Jones, J. M.; Berggren, W. T.; Mitcham, E. R.; Frane, J. L.; Crandall, L. J.; Daigh, C. A.; Conard, K. R.; Piekarczyk, M. S.; Llanas, R. A.; Thomson, J. A. Derivation of Human Embryonic Stem Cells in Defined Conditions. *Nat. Biotechnol.* **2006**, *24*, 185–187.
- (33) Cahan, P.; Daley, G. Q. Origins and Implications of Pluripotent Stem Cell Variability and Heterogeneity. *Nat. Rev. Mol. Cell Biol.* **2013**, *14*, 357–368.
- (34) Constantinescu, D.; Gray, H. L.; Sammak, P. J.; Schatten, G. P.; Csoka, A. B. Lamin A/C Expression is a Marker of Mouse and Human Embryonic Stem Cell Differentiation. *Stem Cells* **2006**, *24*, 177–185.
- (35) Liu, G. H.; Barkho, B. Z.; Ruiz, S.; Diep, D.; Qu, J.; Yang, S. L.; Panopoulos, A. D.; Suzuki, K.; Kurian, L.; Walsh, C.; Thompson, J.; Boue, S.; Fung, H. L.; Sancho-Martinez, I.; Zhang, K.; Yates, J., 3rd; Izpisua Belmonte, J. C. Recapitulation of Premature Ageing with iPSCs from Hutchinson-Gilford Progeria Syndrome. *Nature* **2011**, *472*, 221–225.
- (36) Zuo, B.; Yang, J.; Wang, F.; Wang, L.; Yin, Y.; Dan, J.; Liu, N.; Liu, L. Influences of Lamin A Levels on Induction of Pluripotent Stem cells. *Biol. Open* **2012**, *1*, 1118–1127.
- (37) Eckersley-Maslin, M. A.; Bergmann, J. H.; Lazar, Z.; Spector, D. L. Lamin A/C is Expressed in Pluripotent Mouse Embryonic Stem Cells. *Nucleus* **2013**, *4*, 53–60.
- (38) Liang, G.; Taranova, O.; Xia, K.; Zhang, Y. Butyrate Promotes Induced Pluripotent Stem Cell Generation. *J. Biol. Chem.* **2010**, *285*, 25516–25521.
- (39) Luu, P. L.; Scholer, H. R.; Arauzo-Bravo, M. J. Disclosing the Crosstalk Among DNA Methylation, Transcription Factors, and Histone Marks in Human Pluripotent Cells through Discovery of DNA Methylation Motifs. *Genome Res.* **2013**, *23*, 2013–2029.
- (40) Czabotar, P. E.; Lessene, G.; Strasser, A.; Adams, J. M. Control of Apoptosis by the BCL-2 Protein Family: Implications for Physiology and Therapy. *Nat. Rev. Mol. Cell Biol.* **2013**, *15*, 49–63.
- (41) Ow, Y. P.; Green, D. R.; Hao, Z.; Mak, T. W. Cytochrome c: Functions Beyond Respiration. *Nat. Rev. Mol. Cell Biol.* **2008**, *9*, 532–542.
- (42) Xu, X.; Duan, S.; Yi, F.; Ocampo, A.; Liu, G. H.; Izpisua Belmonte, J. C. Mitochondrial Regulation in Pluripotent Stem Cells. *Cell Metab.* **2013**, *18*, 325–332.
- (43) Wozniak, M. A.; Modzelewska, K.; Kwong, L.; Keely, P. J. Focal Adhesion Regulation of Cell Behavior. *Biochim. Biophys. Acta, Mol. Cell Res.* **2004**, *1692*, 103–119.
- (44) Jaggy, M.; Zhang, P.; Greiner, A. M.; Autenrieth, T. J.; Nedashkivska, V.; Efremov, A. N.; Blattner, C.; Bastmeyer, M.; Levkin, P. A. Hierarchical Micro-Nano Surface Topography Promotes Long-Term Maintenance of Undifferentiated Mouse Embryonic Stem Cells. *Nano Lett.* **2015**, *15*, 7146–7154.
- (45) Dalby, M. J.; Gadegaard, N.; Oreffo, R. O. Harnessing Nanotopography and Integrinmatrix Interactions to Influence Stem Cell Fate. *Nat. Mater.* **2014**, *13*, 558–569.
- (46) Kerr, B. A.; Byzova, T. V. Integrin Alpha V (ITGAV). In *Encyclopedia of Signaling Molecules*; Choi, S., Ed.; Springer: New York, 2012; Vol. 2, pp 949–959.
- (47) Silva, J.; Barrandon, O.; Nichols, J.; Kawaguchi, J.; Theunissen, T. W.; Smith, A. Promotion of Reprogramming to Ground State Pluripotency by Signal Inhibition. *PLoS Biol.* **2008**, *6*, e253.
- (48) Xu, X.; Wang, Q.; Long, Y.; Zhang, R.; Wei, X.; Xing, M.; Gu, H.; Xie, X. Stress-Mediated p38 Activation Promotes Somatic Cell Reprogramming. *Cell Res.* **2013**, *23*, 131–141.